Supporting information for

Interactions of Sub-five-nanometer Diameter Colloidal Palladium Nanoparticles in Solution Investigated via Liquid Cell Transmission Electron Microscopy

Haifeng Wang[a,b,‡], *Xiaoqin Zhou*[b,c,‡], *Yunhui Huang*[*a], *Xin Chen*[*c], *and Chuanhong Jin*[*b,d]

[a] Institute of New Energy for Vehicles, School of Materials Science and Engineering, Tongji University, Shanghai 201804, China.

[b] State Key Laboratory of Silicon Materials, School of Materials Science and Engineering, Zhejiang University, Hangzhou, Zhejiang 310027, China.

[c] Key Laboratory for Ultrafine Materials of Ministry of Education, and Shanghai Key Laboratory of Advanced Polymeric Materials, School of Materials Science and Engineering, East China University of Science and Technology, Shanghai 200237, P. R. China.

[d] Hunan Institute of Advanced Sensing and Information Technology, Xiangtan University, Xiangtan, Hunan 411105, China.

[‡] These authors contributed equally to this work.

Corresponding Authors

[*]Chuanhong Jin, Email: chhjin@zju.edu.cn;

[*]Xin Chen, Email: xinchen73@ecust.edu.cn.

[*]Yunhui Huang, Email: huangyh@tongji.edu.cn.

1. Calculation of the interaction energy

The interaction energy (E) was calculated following the method proposed by Li *et al.*[1]. Generally, E equals to the negative of the sum of the translational and rotational motion energy of NPs and the energy used to overcome the viscosity resistive force and torque, which can be written as:

$$E = -(F_{net}\Delta L + \tau\Delta\theta + \int_0^{\Delta L} F_R dL + \int_0^{\Delta\theta} \tau_R d\theta)$$
$$= -\left(ma\Delta L + \frac{2}{3}mr^2\alpha\Delta\theta + \int_0^{\Delta L}(6\pi\eta r v)dL + \int_0^{\Delta\theta}(8\pi\eta r^3\omega)d\theta \right)$$
$$= -(ma\Delta L + \frac{2}{3}mr^2\alpha\Delta\theta + 4\pi\eta r\sqrt{2(\Delta L)^3 a} + \frac{16}{3}\pi\eta r^3\sqrt{2\alpha(\Delta\theta)^3})$$

where F_{net} is the net force exerted on NP, $F_{net} = ma$, m and a are the mass and instantaneous acceleration of NP, respectively. F_R is the viscosity resistive force from solution, $F_R = 6\pi r\eta v$, *r, η, and v* are the radius of NP, viscosity of liquid layer and velocity of NP, respectively. τ is the torque of NP which can be calculated as $(2/3)mr^2\alpha$, α is the angular acceleration in the unit of rad/s^2. τ_R is the viscosity resistive torque, $\tau_R = 8\pi\eta r^3\omega$, where ω is the angular rate in the unit of rad/s. ΔL and $\Delta\theta$ are the change of inter-NP distance and rotation angle of NP, respectively. For the four items in the calculation formula of E, $-(ma\Delta L + 4\pi\eta r\sqrt{2(\Delta L)^3 a})$ and $-(\frac{2}{3}mr^2\alpha\Delta\theta + \frac{16}{3}\pi\eta r^3\sqrt{2\alpha(\Delta\theta)^3})$ can be classified as the energy related to translation motion (E_{tra}) and the energy related to rotation motion (E_{rot}), respectively.

The viscosity of liquid layer η can be calculated from the Einstein–Stokes equation as:

$$\eta = k_B T / 4\pi r D$$

where k_B is the Boltzmann constant, T denotes the temperature, and D is the diffusion coefficient which can be obtained as following:

$$D = \frac{\left\langle \left| \mathbf{r}(t+\Delta t) - \mathbf{r}(t) \right|^2 \right\rangle_t}{4\Delta t}$$

where the numerator item $\left\langle \left| \mathbf{r}(t+\Delta t) - \mathbf{r}(t) \right|^2 \right\rangle_t$ represents the time averaged mean squared displacement (MSD(Δt))[2, 3] of a NP, $r(t+\Delta t)$ and $r(t)$ represent the positions of

a NP with a time interval Δt, and the average is calculated for all the squared displacements of such position pairs in the trajectory of a NP. Fig. S1 shows the moving trajectory and MSD(Δt) of six individual NPs (denoted as Ps1 to Ps6, respectively) with similar size (~3.5-4.7 nm) in the same observation area. The MSD follows a linear relationship with Δt approximately, and the diffusion coefficients for six NPs are obtained (Table S1), as read from the fitting lines for MSD, which gives an average diffusion coefficient D of 6.4 nm^2/s and 2.2×10^4 Pa·s.

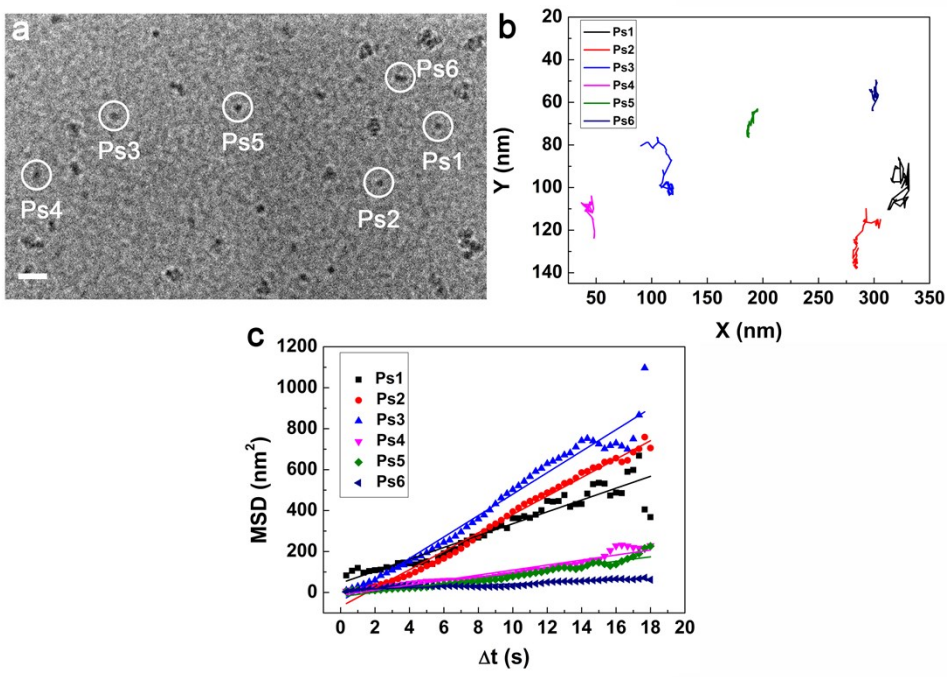

Figure S1 (a) TME images showing the tracked six NPs (Ps1 to Ps6). (b) The moving trajectories of six NPs. (c) The time averaged mean squared displacements (MSD) *vs.* time interval.

Table S1 Diffusion coefficients of NPs in Fig.S1 obtained from line fitting of MSD curve.

NP	D (nm^2/s)
s1	7.3
s2	11.3
s3	13.1
s4	3.1
s5	2.7
s6	0.8

2. Discussion on the validity of the analysis of *E*

An approximation was made during the calculation of the interaction energy E where the contribution from the E_{rot} was omitted, while its validity needs a careful check. In principle, our analysis of E still remains valid, as long as no new minimum point of E is produced when adding E_{rot} to E_{tra}, *i.e.*, $E_{rot} = -(\frac{2}{3}mr^2\alpha\Delta\theta + \frac{16}{3}\pi\eta r^3\sqrt{2\alpha(\Delta\theta)^3})$ should be larger than the smallest energy difference between minimum points of E and non-extreme points. For example, for the E in Fig. 2d, $E_{rot} > -4.6\times10^{-21}$ J, which gives the angle change $\Delta\theta < 0.49$ rad (correspondingly ~28°), assuming the initial angular velocity of the NP is zero. The condition of $\Delta\theta <$ 28° can be satisfied, supposing the NP shared similar rotation motion states with the nanoclusters in the same observation area whose frame to frame $\Delta\theta$ were mainly < 20° (Fig.S2, Movie S4, S5 and S6).

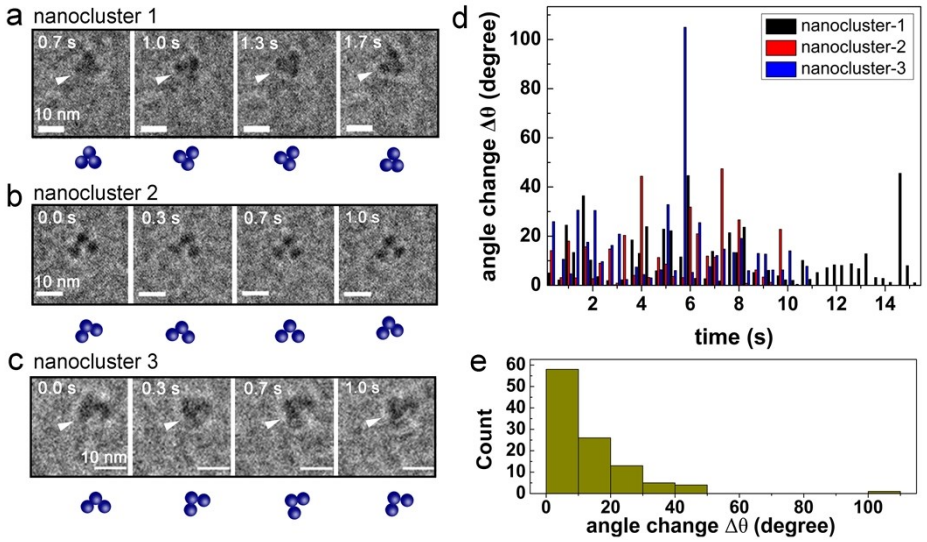

Figure S2 Rotation motion of nanoclusters. (a-c) Time-lapsed TEM image sequences showing the rotation motion of three nanoclusters within the time duration of 1s, respectively. The complete rotation processes of nanoclusters were recorded in the movie S4, S5 and S6, respectively. (c) The $\Delta\theta$ of three nanoclusters with time. (d) The histogram of $\Delta\theta$.

3. Calculation of the vdW interaction and Brownian motion energy and force

3.1 van der Waals (vdW) interaction

The vdW interaction energy (E_{vdW}) acting on the Pd NPs can be determined as following[4]:

$$E_{vdW}(L) = -\frac{A}{6}\left(\frac{2R_1R_2}{(2R_1+2R_2+L)L} + \frac{2R_1R_2}{(2R_1+L)(2R_2+L)} + \ln\frac{(2R_1+2R_2+L)L}{(2R_1+L)(2R_2+L)}\right)$$

where L is the inter-NPs surface to surface separation, R_1 is the apparent radius of a nanocluster, R_2 is the radius of an individual NP obtained from the size distribution (Fig. 1c), and A is the Hamaker constant for Pd NPs in water, which typically ranges from 3.0×10^{-19} to 4.0×10^{-19} J based on the Lifshitz theory[4]. In this study, $A = 4.0\times10^{-19}$ J was chosen for the sub-5 nm Pd NP. The Hamaker constant A may be overestimated in our calculation, as previous works[5, 6] reported that the presence of hydrocarbon chains (CTA^+ in our case) absorbed on NPs would reduce the Hamaker constant and van der Waals interaction force for uncoated NPs.

The vdW interaction force (F_{vdW}) can be obtained as:

$$F_{vdW} = -\frac{\partial E_{vdW}}{\partial L} = -\frac{A}{3}\left[\frac{2R_1R_2(R_1+R_2+L)}{(2R_1+2R_2+L)^2L^2} + \frac{2R_1R_2(R_1+R_2+L)}{(2R_1+L)^2(2R_2+L)^2} - \frac{R_1+R_2+L}{(2R_1+2R_2+L)L} + \frac{R_1+R_2+L}{(2R_1+L)(2R_2+L)}\right]$$

3.2 Brownian motion

Brownian motions of the suspended NPs were driven by the thermal motion of the surrounding fluid molecules[7]. The typical magnitude of Brownian forces F_{Br} can be estimated[8] as $kT/l = \sim10^{-13}$ N, where l denotes a representative length (l = 4.6 nm obtained from the average size analysis); k_B and T stand for the Boltzmann's constant (1.38×10^{-23} J) and the absolute temperature (298 K in our experiments), respectively.

4. Calculation of ionic strength *I*

We calculated the ionic strength of the solution in two hypothesized limiting conditions: the reduction ratio of $PdCl_4^{2-}$ was (a) zero and (b) 100%, respectively. The ionic strength I can be calculated as:

$$I = \frac{1}{2}\sum_{i=1}^{n} c_i q_i^2$$

where c_i and q_i are the concentration and valence of each ion. The c_i and corresponded I in both two conditions were listed in Table S2.

Table S2 concentration of ions and ionic strength of the solution

reduction ratio of $PdCl_4^{2-}$	c($PdCl_4^{2-}$) / mM	c(H^+) / mM	c(Cl^-) / mM	c(Br^-) / mM	*I* /mM
0	0.8	6.3	4.7	0.1	7.2
100%	0	6.3	7.9	0.1	7.2

We then considered the change of the concentration of Cl^- in electron irradiated solution, and its effect on ionic strength and Debye length. The electron radiolysis reactions in the presence of Cl^- were shown in Table S3. As seen, two ion species, hydrochloride ion $ClOH^{\bullet-}$ and chlorine radical ion $Cl_2^{\bullet-}$ were generated, which potentially affected the solution ionic strength and Debye length.

Table S3 The electron radiolysis reactions in presence of Cl^- [9, 10]

No.	Reaction	Reaction constant（L mol^{-1} s^{-1}）
1	$Cl^- + OH^\bullet \rightarrow ClOH^{\bullet-}$	4.3×10^9
2	$ClOH^{\bullet-} \rightarrow Cl^- + OH^\bullet$	6.1×10^9
3	$ClOH^{\bullet-} + H^+ \rightarrow Cl^\bullet + H_2O$	2.1×10^{10}
4	$Cl^\bullet + Cl^- \rightarrow Cl_2^{\bullet-}$	2.1×10^{10}
5	$ClOH^{\bullet-} + e_h^- \rightarrow Cl^- + OH^-$	1.0×10^{10}
6	$Cl_2^{\bullet-} + H^\bullet \rightarrow 2Cl^- + H^+$	8.0×10^9
7	$Cl^\bullet + H^\bullet \rightarrow Cl^- + H^+$	1.0×10^{10}
8	$Cl_2^{\bullet-} + 2e_h^- \rightarrow 2Cl^- + H_2O$	1.0×10^{10}

Supposing the reduction ratio of $PdCl_4^{2-}$ was 0% and all Cl^- in solution transformed into $Cl_2^{\bullet-}$, the resulted ionic strength of solution was 6.0 mM, which gave two times the Debye length $2/\kappa$ = 8.0 nm, about 11% larger than the value of $2/\kappa$ = 7.2 nm obtained assuming the concentration $c(Cl^- + ClOH^{\bullet-} + Cl_2^{\bullet-})$ equaled to the initial concentration of Cl^- in solution. In the limiting condition that the reduction ratio of $PdCl_4^{2-}$ was 100% and all Cl^- in solution transformed into $Cl_2^{\bullet-}$, $2/\kappa$ = 8.5 nm, which was 19% larger than the value of $2/\kappa$ = 7.2.

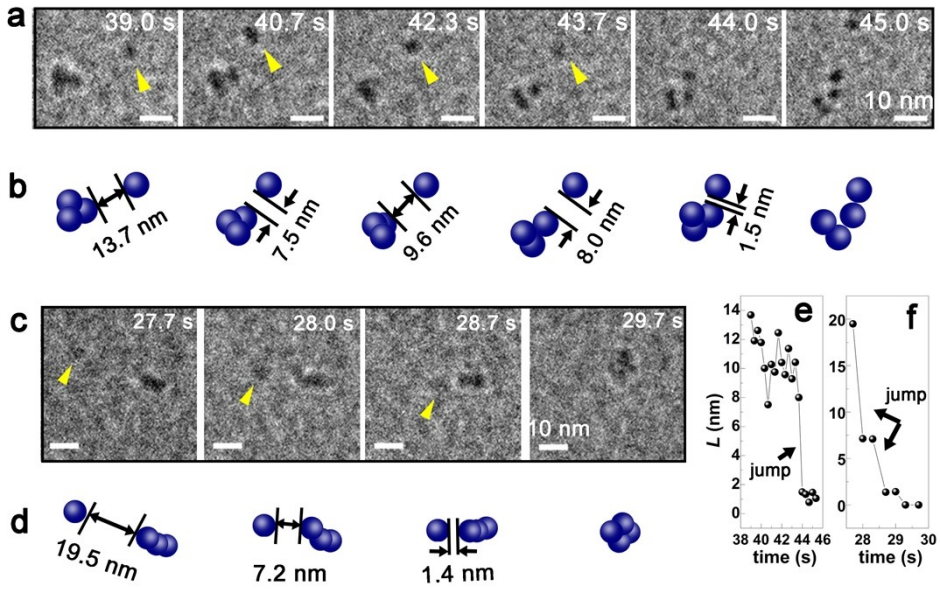

Figure S3 Two cases of the aggregation between NP and nanoclusters. (a, b) and (c, d) Time sequenced TEM images and corresponding schematics of two interaction processes where NPs pointed by yellow triangles jumped toward and then attached to the nanocluters. Electron dose rate: 240 $e^-/Å^2s$. (e) and (f) show the variation of inter-NP distance *L* in (a) and (c), respectively.

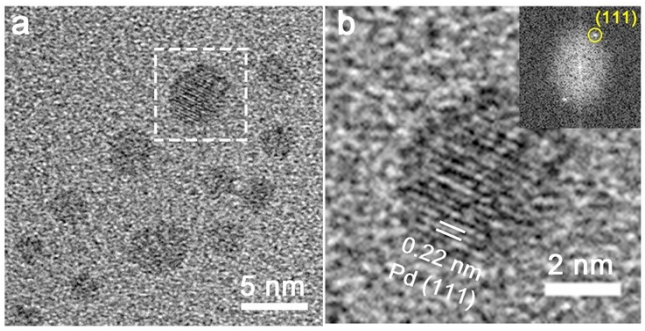

Figure S4 (a) A TEM image of the NPs synthesized *in situ*. (b) The zoom-in image of the NP marked by the white dashed square in (a). The interplanar distance of 0.22 nm corresponds to that of palladium (111) lattice plane. The insert is the fast Fourier transformation of (b).

Movie captions

Movie S1: Growth and aggregation of Pd NPs in solution. Electron dose rate: 240 $e^-/Å^2s$, scale bar: 50 nm.

Movie S2: Aggregation between a Pd dimer and an individual Pd NPs. Electron dose rate: 240 $e^-/Å^2s$, scale bar: 20 nm.

Movie S3: Aggregation between a Pd pentamer (containing five NPs) and an individual Pd NPs. Electron dose rate: 240 $e^-/Å^2s$, scale bar: 20 nm. Note that, the pentamer sometimes appeared as a tetramer (containing four NPs) due to the overlap of NPs.

Movie S4-S6: Rotation motions of three nanocluters. The electron dose for all three movies is 240 $e^-/Å^2s$; scale bar for all three movies is 10 nm.

Reference

1 D. Li, M. H. Nielsen, J. R. Lee, C. Frandsen, J. F. Banfield and J. J. De Yoreo, Direction-specific interactions control crystal growth by oriented attachment, *Science*, 2012, **336**, 1014-1018.

2 H.-G. Liao, L. Cui, S. Whitelam and H. Zheng, Real-time imaging of Pt_3Fe nanorod growth in solution, *Science*, 2012, **336**, 1011-1014.

3 S. W. Chee, Z. Baraissov, N. D. Loh, P. T. Matsudaira and U. Mirsaidov, Desorption-mediated motion of nanoparticles at the liquid–solid interface, *J. Phys. Chem. C*, 2016, **120**, 20462-20470.

4 J. N. Israelachvili, *Intermolecular and surface forces (third edition)*, Academic Press, Boston, 2011.

5 T. Ederth, Computation of lifshitz−van der waals forces between alkylthiol monolayers on gold films, *Langmuir*, 2001, **17**, 3329-3340.

6 J. Galanis, A. Sood, R. Gill and D. Harries, The contribution of capping layer dielectric properties to nanoparticle stability, *Colloid. Surface A*, 2015, **483**, 239-247.

7 T. Li and M. G. Raizen, Brownian motion at short time scales, *Ann. Phys.(Berlin)*, 2013, **525**, 281-295.

8 W. B. Russel, W. B. Russel, D. A. Saville and W. R. Schowalter, *Colloidal dispersions*, Cambridge university press, 1991.

9 G. G. Jayson, B. J. Parsons and A. J. Swallow, Some simple, highly reactive, inorganic chlorine derivatives in aqueous solution. their formation using pulses of radiation and their role in the mechanism of the fricke dosimeter, *J. Chem. Soc., Faraday Trans. 1*, 1973, **69**, 1597-1607.

10 E. Atinault, V. De Waele, U. Schmidhammer, M. Fattahi and M. Mostafavi, Scavenging of e_s^- and OH radicals in concentrated HCl and NaCl aqueous solutions, *Chem. Phys. Lett.*, 2008, **460**, 461-465.